THE GEOLOGICAL SOCIETY OF AMERICA®

Control of silicate weathering by interface-coupled dissolution-precipitation processes at the mineral-solution interface

Encarnación Ruiz-Agudo[1]*, Helen E. King[2], Luis D. Patiño-López[3], Christine V. Putnis[4,5], Thorsten Geisler[6], Carlos Rodriguez-Navarro[1], and Andrew Putnis[4,7]

[1]Departamento de Mineralogía y Petrología, Universidad de Granada, 18071 Granada, Spain
[2]Department of Earth Sciences, Utrecht University, 3584 CD Utrecht, Netherlands
[3]Centro de Investigación Científica de Yucatán, 97302 Mérida, México
[4]Institut für Mineralogie, Universität Münster, 48149 Münster, Germany
[5]Nanochemistry Research Institute, Department of Chemistry, Curtin University, Perth, WA 6845, Australia
[6]Steinmann Institut für Geologie, Mineralogie und Paläontologie, University of Bonn, 53115 Bonn, Germany
[7]The Institute for Geoscience Research (TIGeR), Curtin University, Perth, WA 6845, Australia

ABSTRACT

The mechanism of surface coating formation (the so-called surface altered layers [SALs] or leached layers) during weathering of silicate minerals is controversial and hinges on understanding the saturation state of the fluid at the dissolving mineral surface. Here we present in-situ data on the evolution of the interfacial fluid composition during dissolution of wollastonite ($CaSiO_3$), obtained using interferometry and micro pH and ion-selective electrodes. Steep concentration gradients develop at the mineral interface as soon as it makes contact with the solution. This interfacial fluid becomes supersaturated with respect to amorphous silica that forms a surface coating, limiting fluid access to the mineral surface and hence affecting the dissolution rate. The thickness of the supersaturated zone and the precipitated layer depends on the relative rates of mass transport and surface reaction in the system; this effect could contribute to the discrepancy between dissolution rates measured in the field and in the laboratory. As well, our results have implications for predictions of silicate weathering rates and hence climate evolution, as different assumptions on dissolution mechanisms affect calculations on CO_2 drawdown during weathering and consequent effects on estimates of global mean temperatures.

INTRODUCTION

The observation that the dissolution of most silicate minerals is typically incongruent and results in the formation of silica-rich surface altered layers (SALs), also known as "leached" layers (Casey et al., 1993; Hellmann et al., 2003; Brantley, 2008; Daval et al., 2011), has created major problems in reconciling dissolution models and experimental data, and hence predictions of weathering rates in nature. There is still an open debate regarding the mechanism of SAL formation and its impact on the dissolution kinetics of primary silicates and glasses (Ruiz-Agudo et al., 2012; Schott et al., 2012; Hellmann et al., 2015). The traditionally accepted model suggests that SALs form by the solid-state interdiffusion of protons from the solution and cations in the solid, i.e., a process of element exchange through an otherwise inert silicate structural framework (Casey et al., 1993). However, more recent experimental data challenge this model and support an interface-coupled dissolution-precipitation (ICDP) mechanism as most probable for SAL formation (Hellmann et al., 2003, 2012; Ruiz-Agudo et al., 2012; Putnis, 2014). A common argument against an ICDP mechanism controlling SAL development was that the bulk solution remains undersaturated with respect to the phase forming the SAL (i.e., amorphous silica) (e.g., Brantley, 2008). The counterargument is that during weathering, dissolution of even a few monolayers of the parent surface may result in the fluid layer in contact with the mineral surface becoming supersaturated with respect to this secondary phase (Geisler et al., 2010; Putnis, 2014). This mechanism does not require the bulk fluid to become supersaturated, but this has never been proven experimentally, thereby fueling the existing controversy on the mechanism of SAL formation.

To resolve this paradox, we have monitored the evolution of solution composition during the interaction of wollastonite ($CaSiO_3$) with stagnant and flowing acidic aqueous solutions both qualitatively at a high spatial resolution using real-time Mach-Zehnder phase-shift interferometry and quantitatively using position-sensitive pH and Ca-selective microelectrodes, to determine the saturation state of the fluid at the mineral surface. We have also used an ^{18}O-enriched solution as a tracer to test whether silica is released into solution prior to amorphous silica formation. Wollastonite has been traditionally considered as a model mineral that dissolves incongruently (e.g., Casey et al., 1993; Ruiz-Agudo et al., 2012; Schott et al., 2012). Low-pH conditions were selected to enable measurements in observable time.

METHODS

Batch and flow-through (0–2 mL min^{-1}) wollastonite dissolution experiments were performed at room temperature in open Teflon reactors (30 mL volume) under acidic conditions (pH 1.5). Microelectrodes from Lazar Laboratories (Los Angeles, California, USA) were used for online measurement of pH and free calcium concentration, [Ca], at different distances (0–3.8 mm) from the mineral surface during dissolution experiments. From these data, the time evolution of the maximum saturation state of the solution with respect to wollastonite and amorphous silica was calculated. After the experiments, wollastonite crystals were recovered and observed under a field emission scanning electron microscope (FESEM; Zeiss Supra 40VP) equipped with EDS microanalysis. A Mach-Zehnder phase-shift interferometer was employed for in situ high-resolution qualitative analysis of solution concentration variations during similar dissolution experiments. This technique allows measurement of the refractive index of the solution, which is proportional to its concentration in a particular solute. Finally, batch isotopic tracer experiments during wollastonite reaction in acidic solutions were run at 90 °C for 3 days in 0.1 M HCl solutions. Two experiments, one with water enriched in ^{18}O (67 at% ^{18}O) and one with natural ^{18}O concentrations, were run in parallel to examine the ^{18}O uptake into the amorphous silica. After the experiments, dry wollastonite grains were embedded in epoxy and cross-sectioned

*E-mail: encaruiz@ugr.es

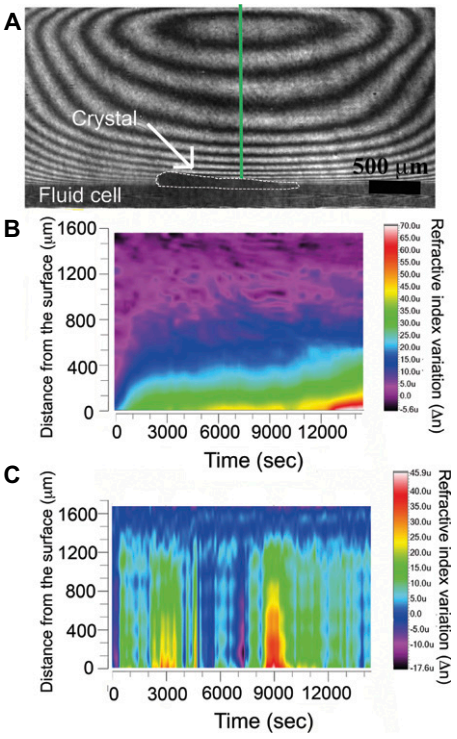

Figure 1. Real-time Mach-Zehnder phase-shift interferometry analysis of wollastonite ($CaSiO_3$) dissolution. A: X-Y image of wollastonite crystal and interference fringes in acidic aqueous solution (pH 1.5, HCl). B,C: Contour maps showing time evolution of solution refractive index in u (units) as function of distance from mineral surface, along profile shown by green line in A, for stagnant and flowing solution, respectively.

for SEM and Raman spectroscopic measurements using a Horiba Scientific LabRam HR800 confocal micro-Raman spectrometer. Further experimental details are provided in the GSA Data Repository[1].

RESULTS AND DISCUSSION

Phase-shift interferometry data and pH and Ca-selective microelectrode measurements (Figs. 1 and 2; Fig. DR1a in the Data Repository) demonstrate that during wollastonite dissolution, large compositional gradients (between 1.2 and 3 mm in thickness) that evolve during the dissolution process are established between fluid at the mineral surface and bulk acidic solutions (pH 1.5) in contact with the mineral. Interestingly, while in batch reactor experiments the gradient increases continuously over time, in flow-through experiments the gradients display periodic variations pointing to time-dependent changes in dissolution rates, consistent with published results (Ruiz-Agudo et al., 2012). Contour maps in Figures 2A and 2B and in Figures DR1a and DR1b depict the time-dependent evolution of pH and [Ca] as a function of distance from the mineral surface. It can be seen that (1) independent of distance from the mineral-fluid interface, [Ca] decreases with reaction time, and (2) [Ca] is highest at the mineral surface. Our previous in situ atomic force microscopy observations (Ruiz-Agudo et al., 2012) strongly suggest congruent dissolution of wollastonite, and thus the initial gradient in [Ca] measured here should also reflect the initial Si concentration gradient. In this study, the formation of etch pits was accompanied by the precipitation of a new phase on the wollastonite surface. This observation demonstrates that silicate dissolution may be transport controlled even though etch pits form on the dissolving surface.

Raman spectra of the SALs confirm that the precipitate is amorphous silica (Fig. 3), characterized by an intense band at 485 cm^{-1} (D_1 band) (Fig. 3B) that reflects the stretching modes of four-membered silicate rings in amorphous SiO_2. All locations within the rim produced during the ^{18}O-enriched experiments showed a 10 cm^{-1} red shift in the D_1 peak in comparison to the ^{16}O-rich experiment, which was confirmed by the same shift of the SiO_4–SiO_4 peak (Fig. 3B). This shift is consistent with ^{18}O incorporation into the amorphous silica structure. By assuming a simple linear relationship between the ^{18}O content and frequency shift we calculate that the observed shift is caused by ~34 at% ^{18}O within the amorphous silica structure. Such high ^{18}O enrichment in the SALs is not consistent with a model involving isotopic exchange between water and silanol and siloxane groups of SALs that formed by solid-state reconstruction of a Ca-leached wollastonite network (Westrich et al., 1989). Hydroxylation of the silica chain during dissolution will lead to an O atom from the water being incorporated into each silica unit. Based on the original solution enrichment of 67 at%, the hydroxylation should thus enrich the silica by 17 at%. Therefore the calculated enrichment indicates that silica was also released into solution where it was free to exchange O atoms with the surrounding water molecules (King et al., 2011).

Our calculations indicate that in the initial stages of the reaction in an unstirred solution, only the solution at the mineral-fluid interface (up to ~1.8 mm from the mineral surface) is supersaturated with respect to amorphous silica (Fig. 2D; Fig. DR2), confirming that its precipitation within this fluid layer is thermodynamically possible and likely, as the nucleation barrier for amorphous silica nucleation is very low. In fact, FESEM-EDS analyses show a porous, homogeneous Si-rich coating on all surfaces of weathered wollastonite crystals (Fig. 3D). For flow-through experiments (1 mL min^{-1}), our

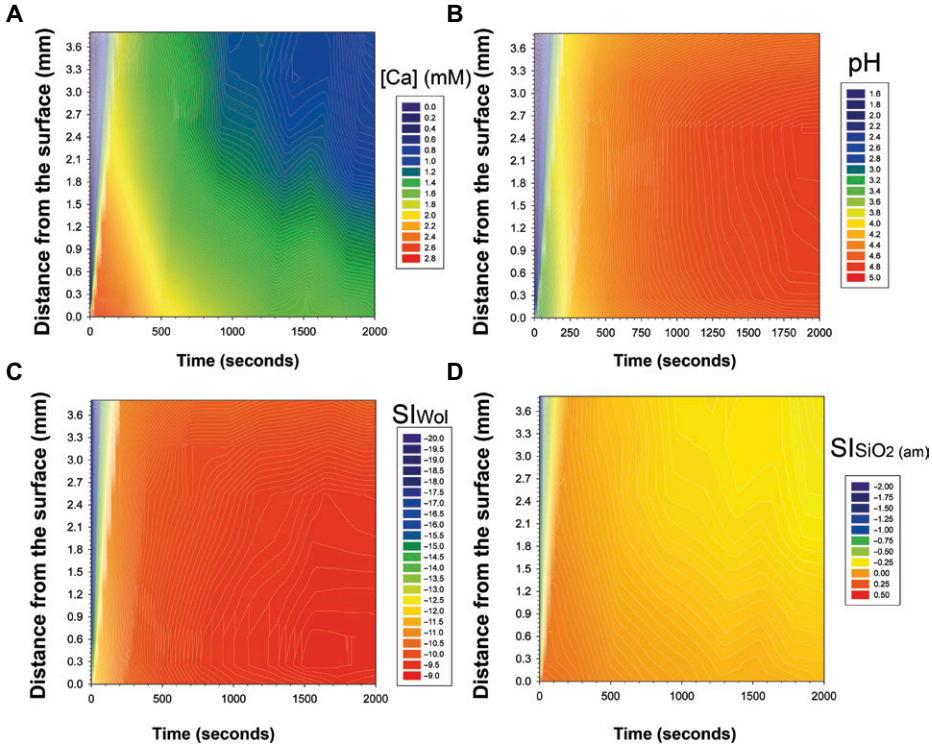

Figure 2. Contour maps showing time evolution of solution free Ca^{2+} concentration ([Ca]) (A), pH (B), and saturation index (SI) with respect to wollastonite ($CaSiO_3$) (C) and amorphous (am) silica (D) during wollastonite batch dissolution experiments in acidic aqueous solution (pH 1.5, HCl).

[1]GSA Data Repository item 2016188, materials and methods, and effect of surface-altered layers on modeling of global temperature and atmospheric CO_2, is available online at www.geosociety.org/pubs/ft2016.htm, or on request from editing@geosociety.org or Documents Secretary, GSA, P.O. Box 9140, Boulder, CO 80301, USA.

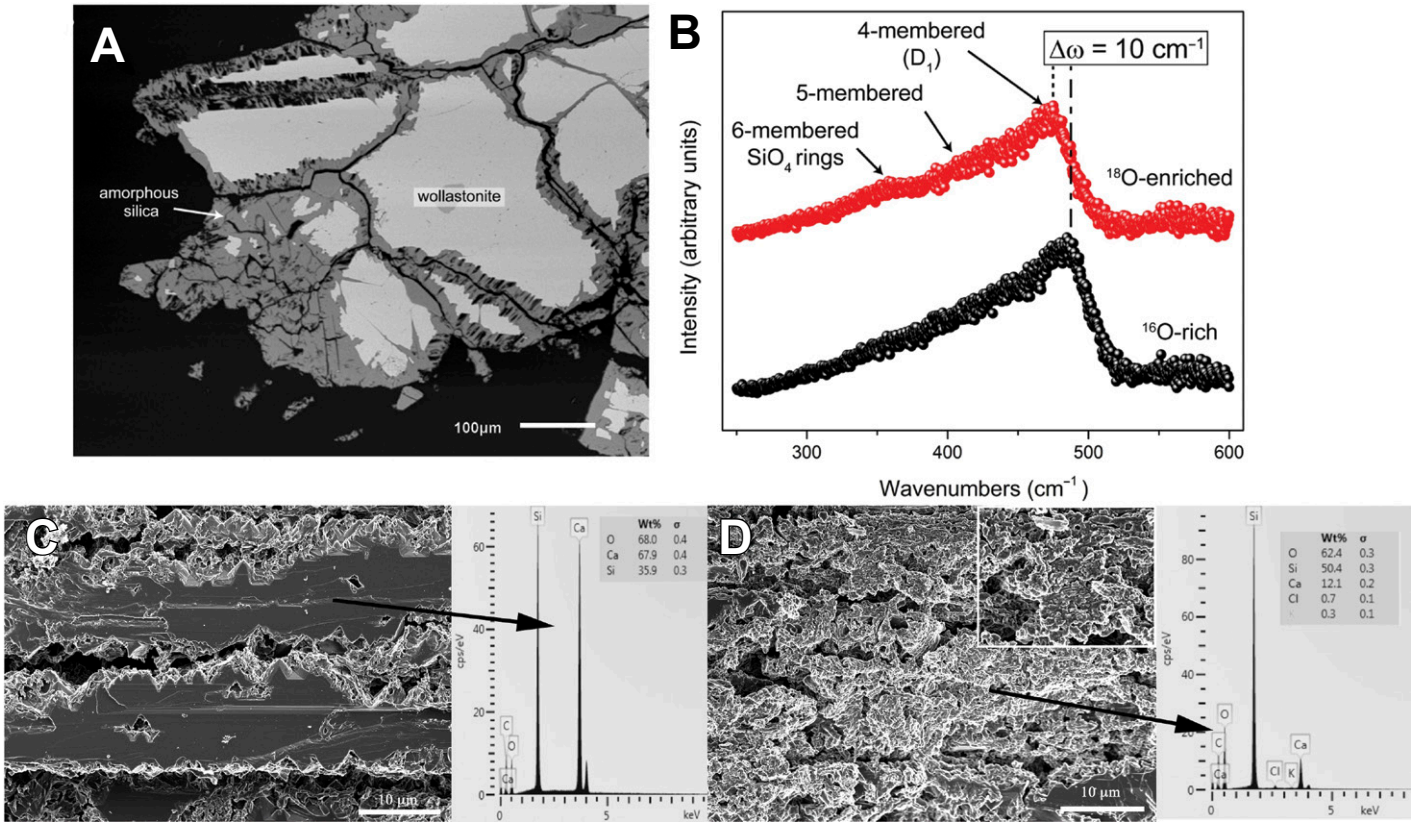

Figure 3. A: Backscattered electron image of cross-section through wollastonite ($CaSiO_3$) crystal reacted with 0.1 M HCl at 90 °C for 3 d. Center corresponds to unreacted wollastonite core, while darker rim corresponds to amorphous silica layer. B: Raman spectra of amorphous silica rim formed in ^{18}O-rich (red) and ^{16}O-rich (black) 0.1 M solution. Δω shows the shift in the 485 cm^{-1} (D1) band. C,D: Secondary electron images of weathered wollastonite surfaces showing crystals dissolved in solution at pH 1.5 and flow rate 2.5 mL min^{-1} (C) and 0 mL min^{-1} (D).

calculations indicate that the solution remains undersaturated with respect to amorphous silica at any reaction time and distance from the surface (Fig. DR1d), and hence an amorphous silica layer would not form. This is consistent with FESEM observations showing intensive dissolution on {100} surfaces via the formation of wide pits with sharp "sawtooth" margins (Fig. 3C) similar to those observed following pyroxene and amphibole weathering under reaction-controlled kinetics (Berner et al., 1980). This provides an explanation for observations that in mixed-flow reactor experiments, dissolution of wollastonite at acidic pH was congruent and SALs did not form (Rimstidt and Dove, 1986).

Our data thus suggest that apparent incongruent dissolution arises when a concentration gradient develops at the mineral interface, allowing supersaturation with respect to the precipitating phase to be reached. This ultimately depends on the relative rates of mass transport and surface reaction in the system, and compositional gradients are generally achieved when the dissolution rate is fast relative to diffusion of dissolved species into the bulk solution. Under conditions of low flow rate–to–solid mass ratio, SALs are thus more likely to develop. Additionally, in our batch experiments the solution remains highly undersaturated with respect to wollastonite after 6500 s of reaction, despite the fact that [Ca] and pH values seem to have reached steady values (Fig. 2). This is interpreted to be due to progressive coverage of the dissolving wollastonite surface by the SAL (Schott et al., 2012), which isolates the unreacted wollastonite surface from "free" fluid. Within the pore system of the SAL, diffusivities are expected to be significantly reduced with respect to the bulk aqueous medium (Daval et al., 2015).

In summary, we propose an ICDP mechanism (Putnis, 2009)—initially controlled by the establishment of a steep compositional gradient at the mineral fluid-interface, and in later stages governed by solute transport through the fluid within the SAL (e.g., Geisler et al., 2015)—as a model for SAL formation. Initially, the diffusion length scale within the SAL is so short that the system is close to surface reaction (stoichiometric dissolution) control. With the development of the SAL, solute transport becomes slower due to an increase in the thickness of the SAL, resulting in a decrease in the overall weathering rate. Steep concentration gradients can initially result when dissolution takes place far from equilibrium at low-pH conditions and/or at low fluid flow rates. Thus thicker silica SALs can form in batch experiments and under acidic conditions compared to those formed in flow-through experiments and under circum-neutral conditions (Brantley, 2008; Daval et al., 2009). During natural weathering, the ratio of effective surface area to fluid flow rate is commonly lower than in laboratory experiments (Velbel, 1993), which could explain the common occurrence of SALs on naturally weathered silicates (e.g., Nugent et al., 1998; Zhu et al., 2006; Nesbitt and Muir, 1988; Banfield and Eggleton, 1990). This would contribute to the apparent discrepancy between weathering rates measured in the laboratory compared to those in nature (Velbel, 1993; Nugent et al., 1998; Zhu et al., 2006).

Chemical weathering and SAL formation under acidic conditions similar to those used in this study take place in many terrestrial environments, including geological CO_2 capture and storage, acid mine drainage, hydrothermal volcanic terrains, or acidic soils (Hellmann et al., 2012). Additionally, SALs can form on naturally weathered minerals under a wide range of pH values (Nugent et al., 1998; Zhu et al., 2006; Nesbitt and Muir, 1988; Banfield and Eggleton, 1990) but are thinner at neutral to basic pH (Hellmann et al., 2012). Thin layers may also eventually show "passivating" effects with the progression of the weathering reaction, due to changes in the compactness of the SAL or its tortuosity. In this respect, Daval et al. (2015)

have shown that diffusivity within SALs formed on wollastonite decreases with dissolution time. Finally, experimental studies on the dissolution of minerals such as forsterite have also reported low activation energy values (Brady, 1991), suggesting transport-controlled kinetics in these cases as well. We thus propose that our model applies to silicate weathering under most physicochemical conditions prevailing on Earth's surface.

IMPLICATIONS

The dependence of SAL formation on flow rate can be easily explained considering ICDP but would be difficult to predict if SALs were formed by a solid-state interdiffusion process. Moreover, solid-state reactions are much slower than dissolution-precipitation reactions, and thus different rate laws should be considered when modeling silicate weathering. The fact that SALs do represent a diffusional barrier has to be taken into account when considering the rate-controlling step during silicate weathering (surface reaction versus transport) for climate modeling purposes. These findings open new ways to better understand the complex interplay between geochemical processes and Earth's climate evolution over geologic time. In particular, we propose that under high-pCO_2 and high-temperature conditions, enhanced vertical drainage associated with a warmer climate should favor reaction-controlled silicate weathering (i.e., absence of SALs) and rapid CO_2 drawdown. Conversely, as CO_2 drawdown progresses after a greenhouse event, the lower pCO_2 and temperature and associated lower runoff and plant productivity should foster the development of SALs (i.e., transport-controlled kinetics), dampening the negative feedback between chemical weathering, pCO_2 and Earth's global temperature.

Finally, quantitative extrapolation of laboratory rates to natural systems is not straightforward, mostly due to differences in the rate-limiting processes controlling weathering. Under fast fluid flow rates, dissolution may be rate limited by the interfacial reaction, thereby displaying a relatively high activation energy, E_a, while lower flow rates or stagnant solutions may result in SAL formation where dissolution is rate limited by transport, thus showing a low E_a. When low E_a is input into existing models that calculate paleotemperature and atmospheric CO_2 levels, the result is higher CO_2 levels and warmer temperatures than those estimated by assuming higher E_a determined in congruent dissolution experiments (Brady, 1991; see the Data Repository).

ACKNOWLEDGMENTS

We acknowledge support from the Spanish Government (grants CGL2015-70642-R and CGL2015-73103-EXP) and the Junta de Andalucía (research group RNM-179 and project P11-RNM-7550). E. Ruiz-Agudo also acknowledges the Spanish Ministry of Economy and Competitiveness for a Ramón y Cajal grant. H.E. King acknowledges funding from a DFG grant (PU153/16-1) and EU Marie Curie International Outgoing Fellowship (PIOF-GA-2012–328731). C.V. Putnis and A. Putnis acknowledge funding from the EU Marie Curie ITNs: CO_2 React; FlowTrans; and Minsc. We thank three anonymous reviewers whose comments improved the manuscript.

REFERENCES CITED

Banfield, J.F., and Eggleton, R.A., 1990, Analytical transmission electron microscope study of plagioclase, muscovite, and K-feldspar weathering: Clays and Clay Minerals, v. 38, p. 77–89, doi:10.1346/CCMN.1990.0380111.

Berner, R.A., Sjöberg, E.L., Velbel, M.A., and Krom, M.D., 1980, Dissolution of pyroxenes and amphiboles during weathering: Science, v. 207, p. 1205–1206, doi:10.1126/science.207.4436.1205.

Brady, P.V., 1991, The effect of silicate weathering on global temperature and atmospheric CO_2: Journal of Geophysical Research, v. 96, p. 18,101–18,106, doi:10.1029/91JB01898.

Brantley, S.L., 2008, Kinetics of mineral dissolution, *in* Brantley, S.L., et al., eds., Kinetics of Water-Rock Interaction: New York, Springer, p. 151–210, doi:10.1007/978-0-387-73563-4_5.

Casey, W.H., Westrich, H.R., Banfield, J.F., Ferruzzi, G., and Arnold, G.W., 1993, Leaching and reconstruction at the surfaces of dissolving chain-silicate minerals: Nature, v. 366, p. 253–256, doi:10.1038/366253a0.

Daval, D., Martinez, I., Guigner, J.M., Hellmann, R., Corvisier, J., Findling, N., Dominici, C., Goffé, B., and Guyot, F., 2009, Mechanism of wollastonite carbonation deduced from micro- to nanometer length scale observations: The American Mineralogist, v. 94, p. 1707–1726, doi:10.2138/am.2009.3294.

Daval, D., et al., 2011, Influence of amorphous silica layer formation on the dissolution rate of olivine at 90 °C and elevated pCO_2: Chemical Geology, v. 284, p. 193–209, doi:10.1016/j.chemgeo.2011.02.021.

Daval, D., Rémusat, L., Bernard, S., Wild, B., Micha, J.S., Rieutord, F., and Fernandez-Martinez, A., 2015, Transport properties of interfacial Si-rich layers formed on silicate minerals during weathering: Implications for environmental concerns: Geophysical Research Abstracts, v. 17, Abs. EGU2015-7678.

Geisler, T., Janssen, A., Scheiter, D., Stephan, T., Berndt, J., and Putnis, A., 2010, Aqueous corrosion of borosilicate glass under acidic conditions: A new corrosion mechanism: Journal of Non-Crystalline Solids, v. 356, p. 1458–1465, doi:10.1016/j.jnoncrysol.2010.04.033.

Geisler, T., Nagel, T., Kilburn, M., Janssen, A., Icenhower, J., Fonseca, R.O.C., Grange, M., and Nemchin, A.A., 2015, The mechanism of borosilicate glass corrosion revisited: Geochimica et Cosmochimica Acta, v. 158, p. 112–129, doi:10.1016/j.gca.2015.02.039.

Hellmann, R., Penisson, J.-M., Hervig, R.L., Thomassin, J.-H., and Abrioux, M.-F., 2003, An EFTEM/HRTEM high-resolution study of the near surface of labradorite feldspar altered at acid pH: Evidence for interfacial dissolution-reprecipitation: Physics and Chemistry of Minerals, v. 30, p. 192–197, doi:10.1007/s00269-003-0308-4.

Hellmann, R., Wirth, R., Daval, D., Barnes, J.-P., Penisson, J.-M., Tisserand, D., Epicier, T., Florin, B., and Hervig, R.L., 2012, Unifying natural and laboratory chemical weathering with interfacial dissolution-reprecipitation: A study based on nanometer-scale chemistry of fluid-silicate interfaces: Chemical Geology, v. 294–295, p. 203–216, doi:10.1016/j.chemgeo.2011.12.002.

Hellmann, R., Cotte, S., Cadel, E., Malladi, S., Karlsson, L.S., Lozano-Perez, S., Cabié, M., and Seyeux, A., 2015, Nanometre-scale evidence for interfacial dissolution-reprecipitation control of silicate glass corrosion: Nature Materials, v. 14, p. 307–311, doi:10.1038/nmat4172.

King, H.E., Plümper, O., Geisler, T., and Putnis, A., 2011, Experimental investigations into the silicification of olivine: Implications for the reaction mechanism and acid neutralization: The American Mineralogist, v. 96, p. 1503–1511, doi:10.2138/am.2011.3779.

Nesbitt, H.W., and Muir, I.J., 1988, SIMS depth profiles of weathered plagioclase and processes affecting dissolved Al and Si in some acidic soil solutions: Nature, v. 334, p. 336–338, doi:10.1038/334336a0.

Nugent, M.A., Brantley, S.L., Pantano, C.G., and Maurice, P.A., 1998, The influence of natural mineral coatings on feldspar weathering: Nature, v. 395, p. 588–591, doi:10.1038/26951.

Putnis, A., 2009, Mineral replacement reactions: Reviews in Mineralogy and Geochemistry, v. 70, p. 87–124, doi:10.2138/rmg.2009.70.3.

Putnis, A., 2014, Why mineral interfaces matter: Science, v. 343, p. 1441–1442, doi:10.1126/science.1250884.

Rimstidt, J.D., and Dove, P.M., 1986, Mineral solution reaction rates in a mixed flow reactor: Wollastonite hydrolysis: Geochimica et Cosmochimica Acta, v. 50, p. 2509–2516, doi:10.1016/0016-7037(86)90033-5.

Ruiz-Agudo, E., Putnis, C.V., Rodriguez-Navarro, C., and Putnis, A., 2012, The mechanism of leached layer formation during chemical weathering of silicate minerals: Geology, v. 40, p. 947–950, doi:10.1130/G33339.1.

Schott, J., Pokrovsky, O.S., Spalla, O., Devreux, F., Gloter, A., and Mielczarski, J.A., 2012, Formation, growth and transformation of leached layers during silicate minerals dissolution: The example of wollastonite: Geochimica et Cosmochimica Acta, v. 98, p. 259–281, doi:10.1016/j.gca.2012.09.030.

Velbel, M.A., 1993, Constancy of silicate-mineral weathering-rate ratios between natural and experimental weathering: Implications for hydrologic control of differences in absolute rates: Chemical Geology, v. 105, p. 89–99, doi:10.1016/0009-2541(93)90120-8.

Westrich, H.R., Casey, W.H., and Arnold, G.W., 1989, Oxygen isotope exchange in the leached layer of labradorite feldspar: Geochimica et Cosmochimica Acta, v. 53, p. 1681–1685, doi:10.1016/0016-7037(89)90252-4.

Zhu, C., Veblen, D.R., Blum, A.E., and Chipera, S.J., 2006, Naturally weathered feldspar surfaces in the Navajo Sandstone aquifer, Black Mesa, Arizona: Electron microscopic characterization: Geochimica et Cosmochimica Acta, v. 70, p. 4600–4616, doi:10.1016/j.gca.2006.07.013.

Manuscript received 1 March 2016
Revised manuscript received 19 May 2016
Manuscript accepted 20 May 2016

Printed in USA